

NELC / TR 2022

NELC / TR 2022

AD A 038708



OVER-THE-HORIZON OPTICAL SCATTER COMMUNICATION IN THE MARINE BOUNDARY LAYER

OTH propagation measurements including path loss and pulse distortion in the blue-green and at $1.06\mu\text{m}$ are presented for use in system design

GC Mooradian, M Geller, R Krautwald, and DH Stephens

28 January 1977

Research and Development, January to December 1976

Prepared for
NAVAL ELECTRONIC SYSTEMS COMMAND

APPROVED FOR PUBLIC RELEASE; DISTRIBUTION IS UNLIMITED

AD NU.

DDC FILE COPY

NAVAL ELECTRONICS LABORATORY CENTER
SAN DIEGO, CALIFORNIA 92152

UNCLASSIFIED

SECURITY CLASSIFICATION OF THIS PAGE (When Data Entered)

REPORT DOCUMENTATION PAGE		READ INSTRUCTIONS BEFORE COMPLETING FORM
1. REPORT NUMBER NELC Technical Report 2022 (TR 2022)	2. GOVT ACCESSION NO. 14/NEC-2022	3. RECIPIENT'S CATALOG NUMBER 14/NEC-2022
4. TITLE (and Subtitle) OVER-THE-HORIZON OPTICAL SCATTER COMMUNICATION IN THE MARINE BOUNDARY LAYER (OTH propagation measurements including path loss and pulse distortion in the blue-green and at 1.06 μm are presented for use in system design)		5. TYPE OF REPORT & PERIOD COVERED Research & Development, 1976 January to December 1976
7. AUTHOR(s) micrometers GC Mooradian, M Geller, R Krautwald, and DH Stephens		6. PERFORMING ORG. REPORT NUMBER
9. PERFORMING ORGANIZATION NAME AND ADDRESS Naval Electronics Laboratory Center San Diego, California 92152		8. CONTRACT OR GRANT NUMBER(s) F21222 XF21222025
11. CONTROLLING OFFICE NAME AND ADDRESS Naval Electronic Systems Command		10. PROGRAM ELEMENT, PROJECT, TASK AREA & WORK UNIT NUMBERS 62721N, F21222, XF21222025 (NELC B195)
14. MONITORING AGENCY NAME & ADDRESS (if different from Controlling Office)		12. REPORT DATE 28 January 1977
		13. NUMBER OF PAGES 18
		15. SECURITY CLASS. (of this report) Unclassified
		15a. DECLASSIFICATION/DOWNGRADING SCHEDULE
16. DISTRIBUTION STATEMENT (of this Report) Approved for public release; distribution is unlimited.		
17. DISTRIBUTION STATEMENT (of the abstract entered in Block 20, if different from Report) DDC APR 27 1976 C		
18. SUPPLEMENTARY NOTES 403 940		
19. KEY WORDS (Continue on reverse side if necessary and identify by block number) Electromagnetic wave transmission Over the horizon detection Telecommunications - Optical systems		
20. ABSTRACT (Continue on reverse side if necessary and identify by block number) Measurements of optical propagation over-the-horizon caused by scattering from normal marine atmospheric aerosols have been made at a range of 40 miles. Path loss, scattered beam angular distributions, and pulse distor- tion have been measured both at 1.06 μm and in the blue-green. Except for anomalies in expected forward scatter function, the results are in reasonable agreement with the propagation model. Based upon results of the propagation model and experimental results, communications system performance is determined using existing components. Design and construction of a one-way communication link between NELC and San Clemente Island (128 km) are in progress. micrometers		

DD FORM 1 JAN 73 1473

EDITION OF 1 NOV 65 IS OBSOLETE
S/N 0102-LF 014-6601

UNCLASSIFIED

SECURITY CLASSIFICATION OF THIS PAGE (When Data Entered)

OBJECTIVE

Measure the engineering propagation parameters of an optical scatter channel link necessary for quantifying and designing an over-the-horizon optical communication system.

RESULTS

Measurements of propagation by scattering over the horizon caused by marine aerosols have been made for a 40-mile link between NELC and Camp Pendleton. It was shown that:

1. For high visibility conditions (greater than 10 miles), the path loss for visible radiation was nominally about 100 dB (received power divided by transmitted power).*
2. When atmospheric ducting occurs, such as in a Santa Ana, an additional 20 dB or more of optical signal can be expected.
3. For this propagation length, there was no evidence of pulse distortion at either 0.53 or 1.06 μm .
4. The path loss at 1.06 μm was about 20 dB less than at 0.53 μm for identical propagation paths.
5. Electrical signal-to-noise ratios of greater than 90 dB are measured in the 1.06- μm channel (day or night).
6. The multiple scattering model was in better agreement with the experimental data than the single scattering model.
7. The off-axis energy in azimuth of the scattered beam is very sharply peaked in the forward direction. The extent of this effect implies that the forward scattering function could be approximately 100 times that expected.

RECOMMENDATIONS

1. Continue to measure the path loss and pulse dispersion for a large variety of visibility conditions, and for moderate rainfall for this 40-mile propagation path. Repeat these measurements for an 80-mile marine atmosphere path.
2. Investigate the predicted enhancement of received signal with transmitter elevation angle for the 80-mile path.
3. Repeat the above measurements using the base of clouds as scattering centers.

ADMINISTRATIVE INFORMATION

Work was performed under 62721N, F21222, XF21222025 (NELC B195) by the EO/Optics Division. The report covers work done from January to December 1976 and was approved for publication 28 January 1977.

*1 mi = approx 1.6 km

CONTENTS

INTRODUCTION . . .	page 3
ELOS OPTICAL COMMUNICATIONS . . .	3
EXPERIMENTAL RESULTS . . .	5
A. Propagation of CW Radiation . . .	6
B. Propagation of Pulsed Radiation . . .	12
ANALYSIS OF PROPAGATION RESULTS . . .	16
SUMMARY . . .	17
REFERENCES . . .	18

64

TABLE

1. Comparison between Experiment and Theories . . . page 12

FIGURES

1. Performance characteristics of ELOS . . . page 5
2. Propagation path for OTH scattering channel . . . 6
3. Synchronous transmitter for cw measurements . . . 7
4. Synchronous detector for cw measurements . . . 7
5. Ducted beam . . . 8
6. Transmitter elevated 0.5° . . . 8
7. Transmitter elevated 0.75° . . . 8
8. Path loss measurements of 15 January 1976 . . . 10
9. Path loss measurements of 21 January 1976 . . . 10
10. Path loss measurements of 28 January 1976 . . . 11
11. Path loss measurements of 25 February 1976 . . . 11
12. Schematic of dual wavelength transmitter . . . 13
13. Schematic of dual wavelength receiver . . . 13
14. Path loss measurements of 30 September 1976 (elevation scan) . . . 14
15. Path loss measurements of 30 September 1976 (azimuth scan) . . . 14
16. Path loss measurements of 5 November 1976 . . . 15
17. New propagation path . . . 15

INTRODUCTION

Current Navy operational communications systems suffer from a number of problems. There is no operational communications system which is not significantly susceptible to jamming, intercept, spoofing, and direction-finding. Further, current communications systems significantly increase Fleet vulnerability to the threat of ARM (antiradiation missiles). Lastly, the existing systems suffer from limited data rates, spectrum crowding, high cost, large size, excessive weight, high power requirements, etc. Several attempts at solving these problems in the rf spectrum are being carried out. In addition, it appears that optical communications systems have great promise in solving these problems for many applications (ref 1). This report discusses one of the optical communications systems being developed at NELC: the ELOS (extended line of sight) optical communications system. This system addresses the requirement for exchange of tactical data between ships, both to the horizon and beyond. The effects of the atmosphere in the marine boundary layer represent the primary limitation to system performance and are addressed here.

ELOS OPTICAL COMMUNICATIONS

The ELOS optical communications system addresses exchange of tactical information to beyond line-of-sight ranges for the control of task force units. While the ELOS system will most likely be limited to voice bandwidths, the application of this system as an antijam, low-probability-of-intercept (AJ, LPI) augmentation of hf techniques will prove extremely valuable.

A detailed, comprehensive analysis of extended line-of-sight optical communications has been completed (ref 2). Links were studied utilizing both relay platforms and over-the-horizon forward scatter from aerosols (both marine aerosol haze and clouds). An in-depth review of the state of the art and near-term future advances in system component performance was included, covering lasers, filters, photodetectors, pointing and tracking systems, and platforms.

One result of this analysis was an analytical model for over-the-horizon optical scatter propagation, based upon both the single and multiple scattering approximation. The model appears to be in reasonable agreement with previously available field data for over-the-horizon propagation (ref 3).

Based on the use of systems composed of state-of-the-art (1976) components, the following conclusions were drawn (ref 2, 4):

1. The operating wavelength should be in the 1-3- μ m range for both links.
2. Both relay and scatter over-the-horizon data links can use the same shipboard system.

¹ Atmospheric and Space Optical Communications for Naval Applications, Proceedings of 6th DoD Conference on Laser Technology, GC Mooradian, March 1974

² NELC TR 1988, Extended Line of Sight Optical Communications Study, GC Mooradian, VJ Adrian, PH Levine, and WR Stone, June 1976

³ NRL Report 6152, Experimental Observations of Forward Scattering of Light in the Lower Atmosphere, JA Curcio and LF Drummeter, Jr, 30 September, 1964

⁴ Over the Horizon Optical Communications Channel, Proceedings of Workshop on Remote Sensing of the Marine Boundary Layer, Vail, Colorado, GC Mooradian, M Geller, GJ Barstow, KE Davies, August 1976

3. Significant performance advantages can be achieved by exploiting propagation characteristics. These include:
 - a. Use of a vertical fan beam or optimally elevated beams in a scatter link at large ranges.
 - b. Positioning the relay platform at a high altitude to take advantage of the decrease in path loss caused by the vertical falloff in aerosol concentration.
4. Pulse stretching, which becomes significant at ranges beyond 100 km, limits usable data rate, reduces "peak" power of received pulses, and restricts modulation format.
5. Models for the optical scattering channel must include the following:
 - a. Vertical exponential decrease in aerosol concentration and attenuation coefficient.
 - b. Vertical decrease in index of refraction. The simplest approximation is to replace the radius of the earth in the model by the "4/3 radius" (modeling of temperature inversions would be desirable).
 - c. Two modes of propagation: single and multiple scattering. Contrary to intuition, the former dominates at longer ranges and the latter at shorter ranges.

The primary factor which determines the percentage of time communication over a given distance at a given bit rate can be achieved is meteorological visibility. Statistical studies of the occurrence of visibilities greater than a given value are available (ref 5, 6). When this information is combined with performance characteristics of a typical system, both range and link availability can be determined. Figure 1 shows the performance of a communication link based upon the results of the propagation model fit to experimental data. For voice data rates, the transmitter is a pulsed Nd:YAG laser emitting 2.5 MW peak power pulses at 1.06 micrometres with an average power of 10 watts. Note that for a marine atmosphere and visibility as low as 5 miles, the communication range is approximately 42 miles.* For visibility of 10 miles, the range is increased to 91 miles. For 20-mile visibility, the range increases to 205 miles. For teletype data rates and the same average power laser, the ranges become 51 miles, 113 miles, and 261 miles, respectively. On a worldwide basis, visibilities greater than 5 miles occur approximately 85% of the time, and visibilities greater than 10 miles approximately 70%. This link availability for a given range is not substantially different from that provided by conventional hf techniques. The communications ranges can be considerably greater at night and whenever low clouds occur to provide a scattering layer. It is important to note that areas of operation with lower average visibility (eg, the North Atlantic) also have a high occurrence of low cloud cover; and that some areas of high operational interest (eg, the Western Pacific and the Mediterranean) consistently permit greater ranges and higher availabilities. Interpretation of the visibility data on range, data rate, and availability is being continued.

⁵Marine Weather of the World, McDonnell Douglas Report F-063, June 1968

⁶NWC, China Lake, TN 4056-16, Weather Effects on Infrared Systems for Point Defense, FE Nicodemus, May 1972

*1 mi = approx 1.6 km

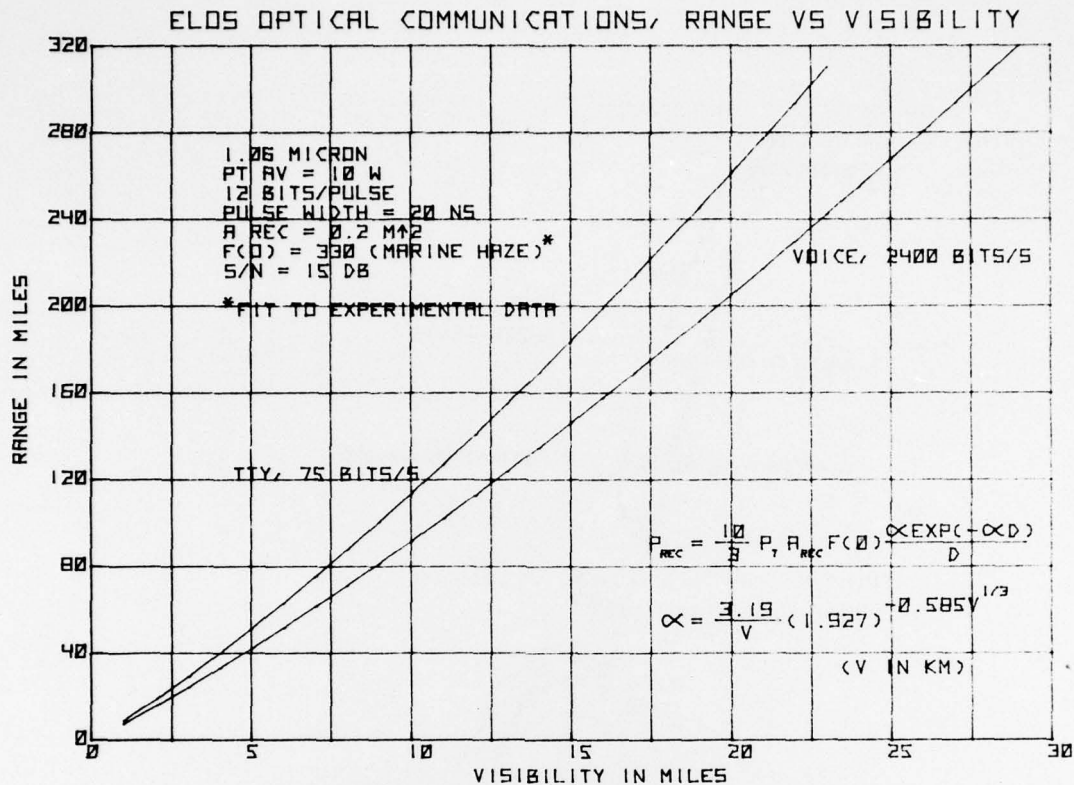


Figure 1. Performance characteristics of ELOS.

EXPERIMENTAL RESULTS

To verify the propagation model developed in reference [2], it was necessary to measure the following scatter channel characteristics during each experimental run:

1. The integrated path loss over the range
2. The angular brightness distribution of the source as seen by the receiver
3. The magnitude of the pulse stretching

These propagation parameters depend critically on both the atmospheric visibility, and the elevation/azimuthal angles of the receiver. In the following section, we will describe recent experimental results derived from an over-the-horizon propagation link between San Diego and Oceanside, California. For this experiment, the integrated path loss (received power divided by transmitted power) was measured using the 514.5-nm line of a 1-watt argon laser, and the 532-nm and 1.06- μm lines of a Q-switched Nd:YAG laser. In the latter, both wavelengths transversed the identical propagation path.

The scattering channel selected was a 39-mile path, almost all of which is over the ocean. The transmitter was at NELC in Point Loma. The receiver was on the beach at the Marine Base at Camp Pendleton. The geometric horizon was 25 miles from the transmitter for the CW experiments and 12 miles for the pulsed. A map presenting details of the propagation path is shown in figure 2.

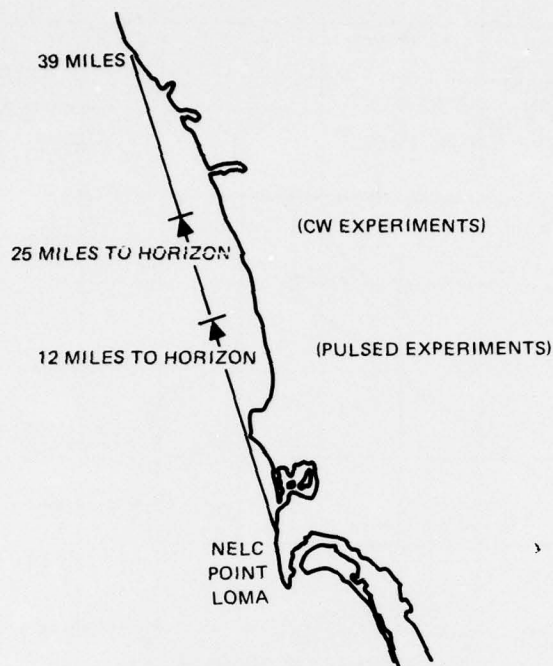


Figure 2. Propagation path for OTH scattering channel.

A. PROPAGATION OF CW RADIATION

A synchronous transmitter was used for the cw measurements (fig 3). A cw argon ion laser emitting about 1 watt at 514.5 nm was chopped at 3 kHz and aimed very accurately in the direction of the site at Camp Pendleton. An electrical signal, synchronized with the chopping frequency, was also sent to Camp Pendleton via a standard telephone line.

The receiver at Camp Pendleton (fig 4) collected the optical chopped signal with an 8-inch-diameter telescope.* The radiation was detected by an S-20 RCA 7265 photomultiplier. The synchronous signal was received from the telephone and, with the received signal, was fed into a PAR lock-in amplifier. This type of synchronous detection permitted the measurement of signals as small as 10^{-14} watt.

Figure 5 is a photograph at nighttime of the coastline from Pendleton looking southward to the source. The transmitter is pointed directly at the geometric horizon. As there was a strong temperature inversion this night (21 January 1976), the direct beam, ducted by this refractive index anomaly, is clearly visible.

Figure 6 is the same view with the transmitter elevated 0.5 degree from the horizon. Superimposed on this photograph is an angular scale to obtain an estimate of the angular size of the source.

Figure 7 is another photograph of the same view with the transmitter elevated 0.75 degree above the horizon.

* 1 in = 25.4 mm

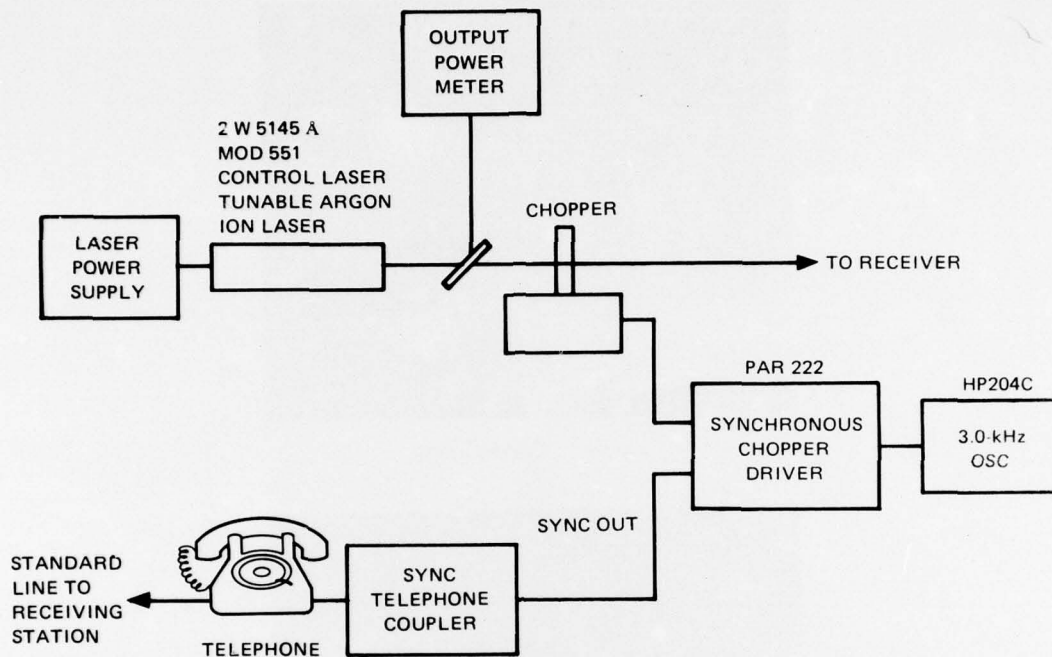


Figure 3. Synchronous transmitter for cw measurements.

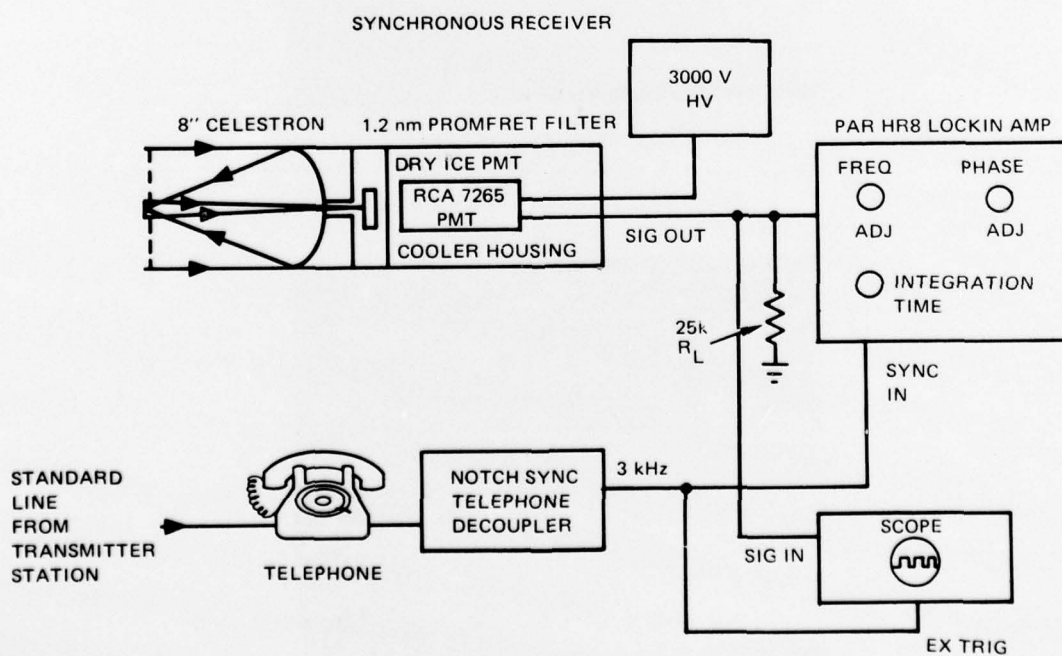


Figure 4. Synchronous detector for cw measurements.



Figure 5. Ducted beam.

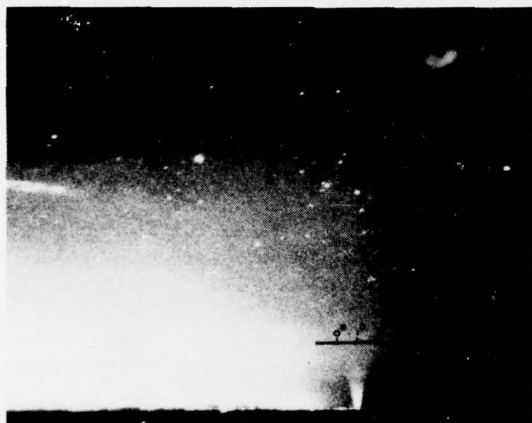


Figure 6. Transmitter elevated 0.5° .

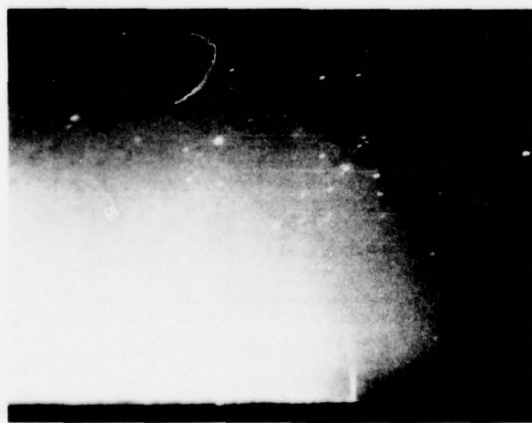


Figure 7. Transmitter elevated 0.75° .

Figure 8 shows the path loss as a function of transmission elevation angle. The vertical axis is the path attenuation in dB: the power received divided by the power transmitted. The path loss for the ducted beam is -83 dB. On the scale used, this data point would be outside the boundary of the graph. Part of this path loss, 51 dB, is due to the loss in beam spreading. The remaining 32 dB is from the loss of energy from the extinction coefficient integrated over this 63-kilometre path.

This enables a calculation of an integrated extinction coefficient of 0.115 km^{-1} to be made for this very long path. This method of determining the integrated extinction coefficient is extremely valuable as visometer and transmissometer measurements disagreed severely. This night only four data points were obtained, when the telephone failed. With sync information gone, no further data were obtained. Note on the right-hand side of the figure the pertinent data are stated: PT is the transmitted power, THETA D is the beam divergence, D REC is the receiver diameter, FOV is the field of view of the receiver, R is the propagation path, VIS is the visibility as calculated from the extinction coefficient, BETA is the extinction coefficient, H TRANS is the height of the transmitter, and H REC is the height of the receiver above sea level.

Figure 9 contains data taken on the same night of the photographs of figures 5-7. The night was remarkably clear from a strong Santa Ana condition. Note that the small value of ducting loss calculates into a visibility of 92 kilometres.

Figure 10 is another data set later in the month of January. This was a very clear night, and the ducted beam was clearly visible to the eye.

The last data set (fig 11) was taken about a month later under conditions more normal to the California coast. There was no temperature inversion, so the direct, unscattered beam was not observed. For all the four points of data, the beam was not visually seen.

The occurrence of a ducting condition is determined two ways by analyzing the data. First, a large decrease in signal level is observed when the transmitter elevation angle is increased beyond about one beam width. This change is approximately -20 dB. Second, the received ducted signal exhibits rapid large amplitude variation, characteristic of scintillation, when the transmitter is pointed at the horizon. When the transmitter beam is elevated, and a scatter condition predominates, the effective radiating volume increases by orders of magnitude (aperture averaging) and amplitude variations of the signal are very small, typically less than a few percent.

The experimental and theoretical values are compared in table 1. The column labeled EXPERIMENT is the path loss with the transmitter pointed about one beam diameter above the horizon to ensure that none of the energy is being ducted to the receiver. The next column, SGL SCATT, gives the values from the single scattering model. The column next to this one, ERROR, gives the difference between the experiment and the single scattering theory. Note that there are large differences from 16 to 30 dB. The next column, MULT SCATT, gives the results from the theory of multiple scattering. A comparison between this column and the experimental values indicates better agreement, with the differences clustered around -19 dB. An analysis of these results is given later.

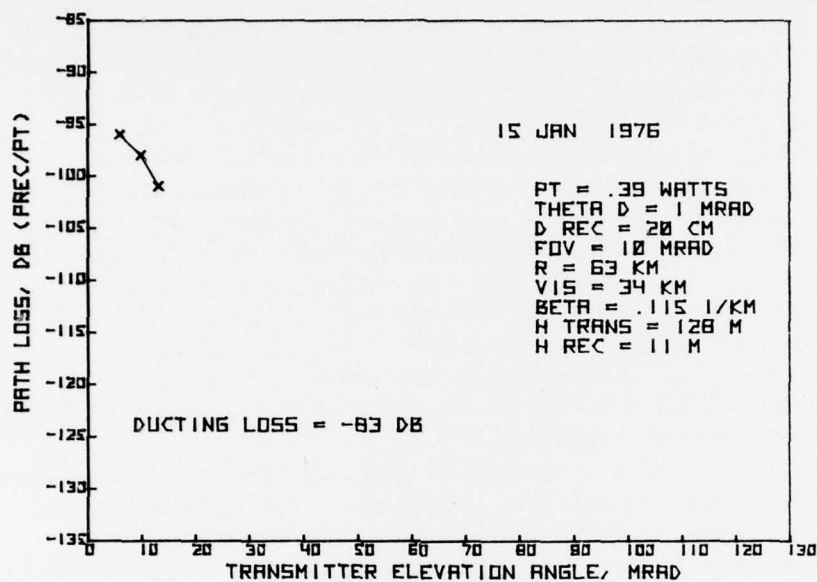


Figure 8. Path loss measurements of 15 January 1976.

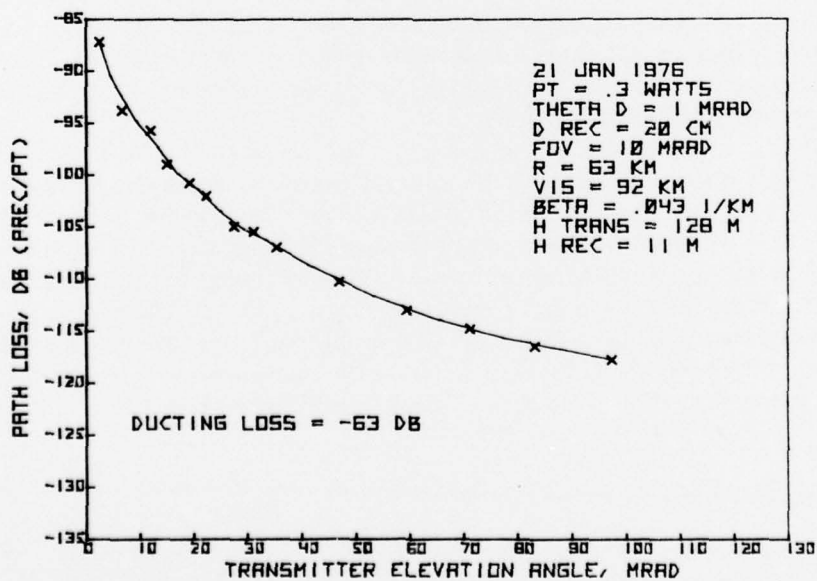


Figure 9. Path loss measurements of 21 January 1976.

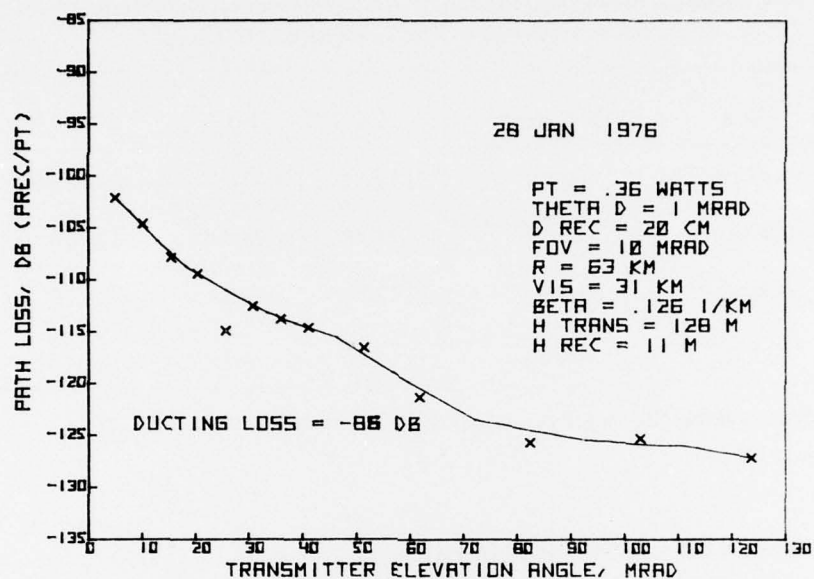


Figure 10. Path loss measurements of 28 January 1976.

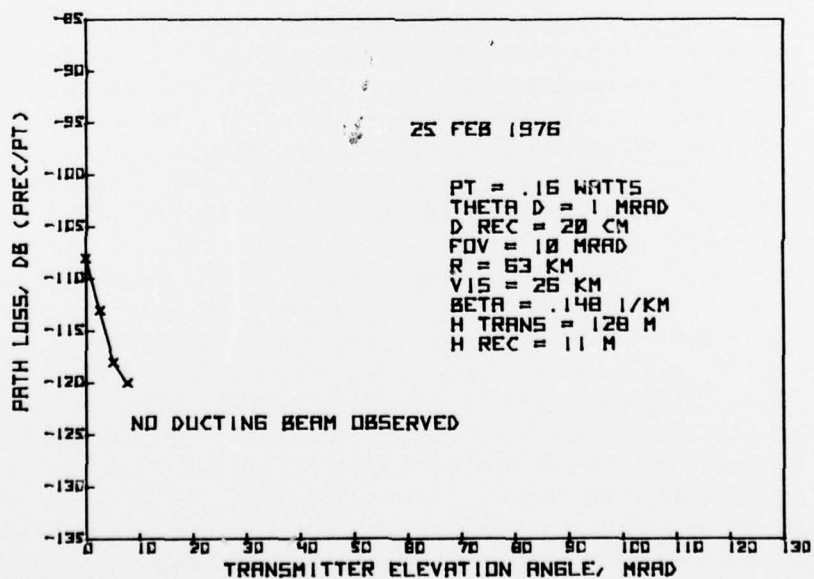


Figure 11. Path loss measurements of 25 February 1976.

TABLE 1. COMPARISON BETWEEN EXPERIMENT AND THEORIES.

Comparison of both single scattering and multiple scattering theoretical models to experimental results over 63-km OTH range.

Date	Beta	Experiment*	SGL SCATT **	Error	MULT SCATT**	Error
1/15/76	0.115 km^{-1}	-96 dB	-117.5 dB	-21.5 dB	-118.5 dB	-22.5 dB
1/21/76	0.043 km^{-1}	-86 dB	-114.7 dB	-28.7 dB	-103 dB	-17 dB
1/28/76	0.126 km^{-1}	-102 dB	-118 dB	-16 dB	-121 dB	-19 dB
2/25/76	0.148 km^{-1}	-108 dB	-119.4 dB	-11.4 dB	-126.5 dB	-18.5 dB

* Measurement of path loss (P_{RCVR}/P_{XMTR}) at transmitter elevation angle of $\sim 3 \text{ mrad}$.

** Assuming $f(0) = 10.3$

B. PROPAGATION OF PULSED RADIATION

The next set of experiments measured both the path loss and the pulse spreading in this type of scatter channel. The transmitter is a pulsed Nd(YAG) laser emitting 20-ns pulses both at the fundamental at 1.06 micrometres and the first harmonic at 532 nm (fig 12). Both wavelengths traverse the same propagation path to the receiver. The radiation is accurately pointed to Camp Pendleton with the aid of a sighting hole near the laser and a sighting mark 50 feet from the laser. The exact positions of these aiming aids were determined by a surveyor. The peak powers of the 1.06- μm and the first-harmonic beams are measured by pyroelectric pulsed energy detectors. Accurate timing of the onset of the pulse at the receiver was obtained by two rubidium clocks. These were synchronized at the start of each experiment. One clock in this figure is shown sending a sync pulse to trigger the laser power supply. The other rubidium standard clock is shown in figure 13. A sync pulse from this clock, delayed for 350 μs to account for the time of flight of the beam, initiates the Biomation digitizers. The two wavelengths, 532 nm and 1.06 μm , are collected by an 8-inch telescope receiver. The two beams are separated by a dichroic beamsplitter, detected, amplified, digitized, and recorded. Real-time displays of the pulse shapes are shown on the oscilloscopes and polaroid photographs taken.

Figures 14 and 15 show the path loss as a function of transmitter elevation and scan angle at a wavelength of 532 nm. The 1.06- μm receiver was not operating during this test. It is important to note that the off-axis energy in azimuth is very sharply peaked in the forward direction (much more so than predicted by standard forward scattering functions). This has important implications for determining LPI and AJ levels. Figure 16 shows the path loss at the two wavelengths of 532 nm and 1.06 μm through the identical atmosphere. As predicted by the model, the 1.06- μm channel has approximately 20-dB less attenuation than the 532-nm channel for these atmospheric conditions and range. The electrical signal-to-noise ratio of the 1.06- μm channel was approximately 90 dB, even in daytime operation. In all these measurements there was no pulse stretching or distortion measured.

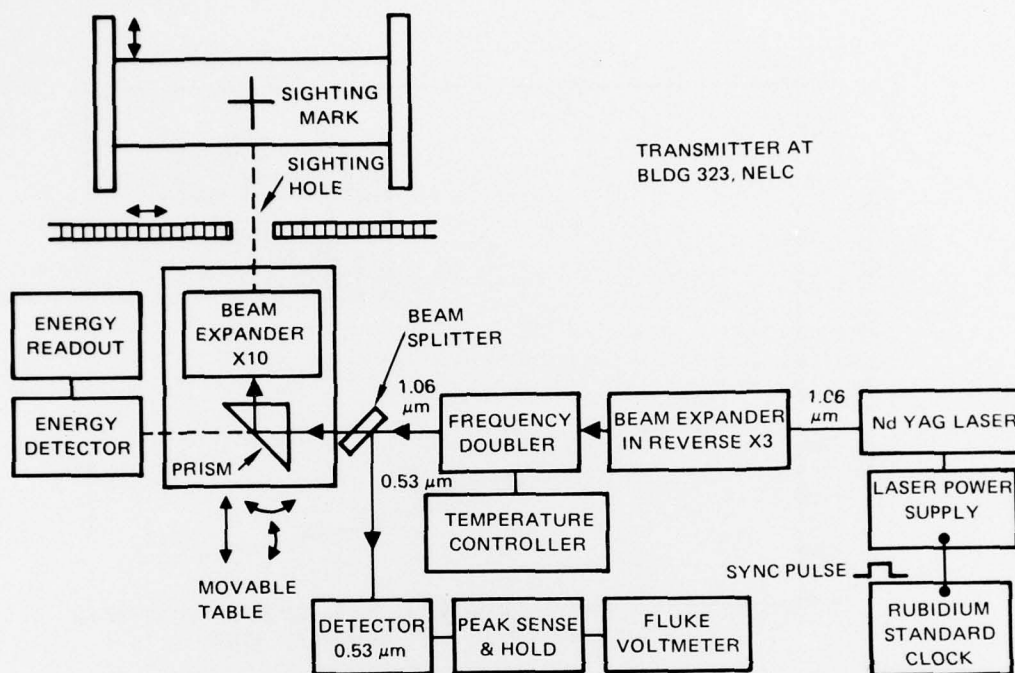


Figure 12. Schematic of dual wavelength transmitter.

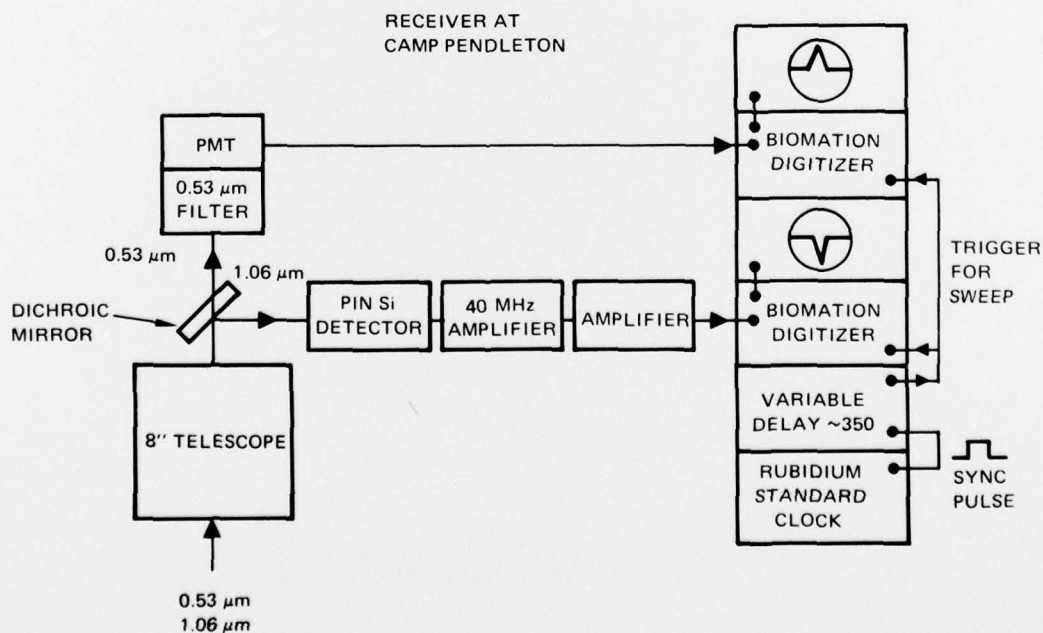


Figure 13. Schematic of dual wavelength receiver.

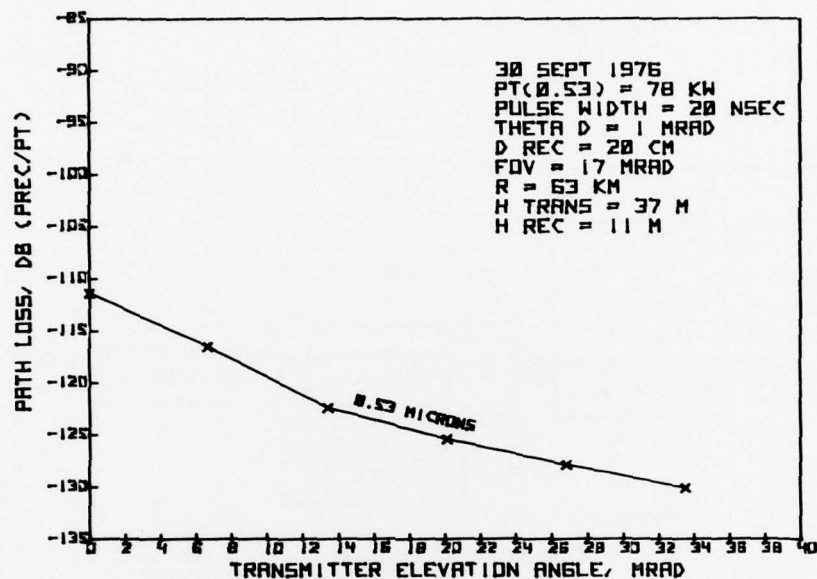


Figure 14. Path loss measurements of 30 September 1976 (elevation scan).

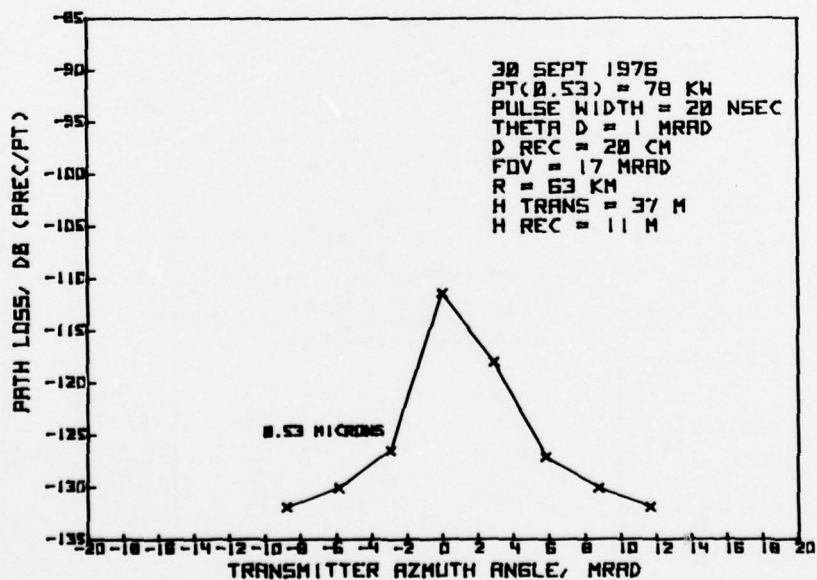


Figure 15. Path loss measurements of 30 September 1976 (azimuth scan).

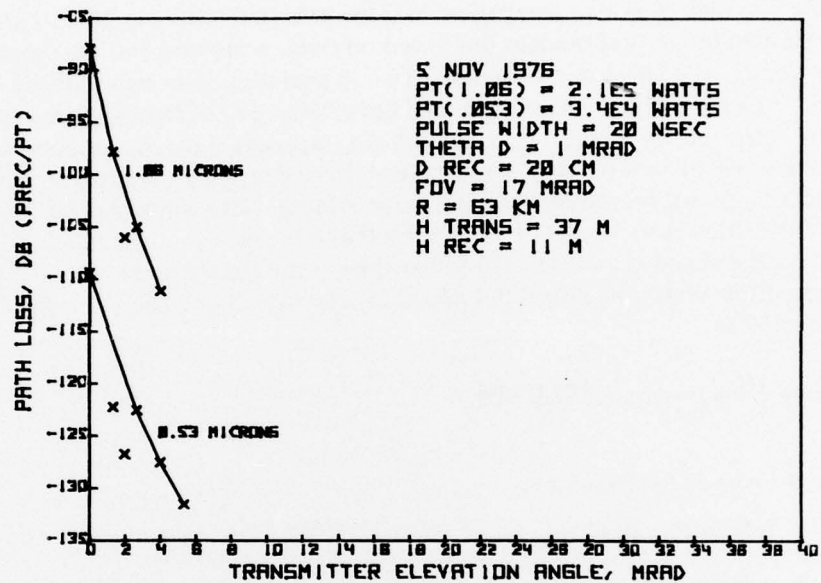


Figure 16. Path loss measurements of 5 November 1976.

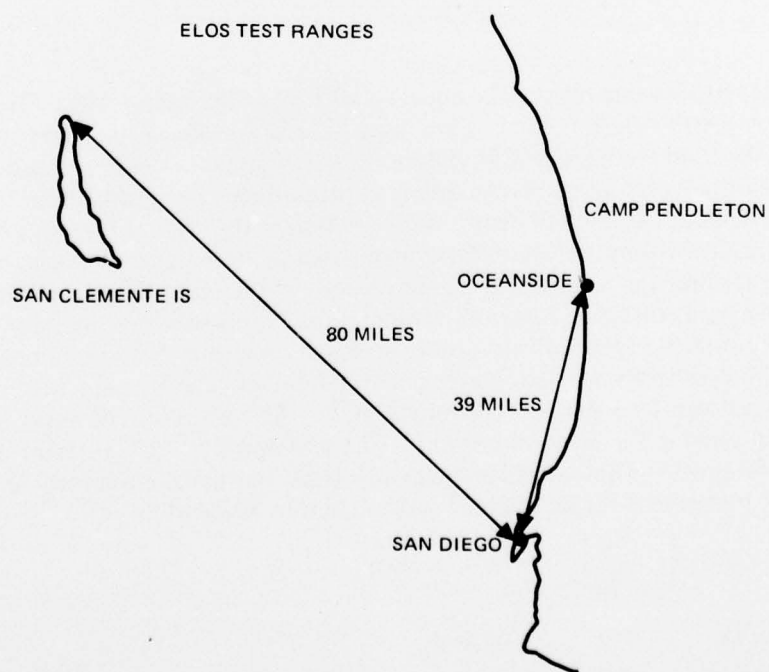


Figure 17. New propagation path.

ANALYSIS OF PROPAGATION RESULTS

In the previous section, a comparison was made between the cw OTH experimental results and the two theoretical models, one based on single scattering and the other on multiple scattering, developed in reference 2. Two important points were evident from that comparison: (1) The multiple scattering model did a better job of tracking the experimental data than the single scatter model. This was not too surprising since the propagation link's optical thickness was always within the multiple scattering regime. (2) Both models consistently under predicted the actual path loss measurement. This was rather surprising. The purpose of this section is to discuss this latter result and to show that the reason for the discrepancy lies in the assumed value of $f(0)$ rather than in the theory itself.

The multiple scattering model developed in reference 2 gave the normalized received power to be equal to

$$\frac{P_{\text{rec}}}{P_t} \approx \frac{10}{3} A_{\text{rec}} f(0) \frac{\beta \exp(-\beta R)}{R},$$

$P_{\text{rec}} \equiv$ received optical power

$P_t \equiv$ transmitted peak power

$A_{\text{rec}} \equiv$ receiver area

$f(0) \equiv$ forward scatter function at 0°

$\beta \equiv$ extinction coefficient

$R \equiv$ range

The parameter $f(0)$ was assumed to be equal to 10.3; the value computed by Deirmendjian for an aerosol distribution he called "water haze M" (ref 7). Recently, it has been shown (ref 8) that the Deirmendjian haze M underestimates the number of large particles contained in a maritime aerosol by several orders of magnitude. The inclusion of several large ($>10\mu\text{m}$) particles in the model's distribution could have the effect of peaking the forward scattering function without an appreciable increase in the value of the extinction coefficient.

The experimental results of the azimuth scan of the transmitter also lead one to suspect the forward scattering function. From figure 15 it is seen that the received power is very sharply peaked in the forward direction, much more than that predicted by the phase function derived from a Deirmendjian haze M model. For this function, the scatter cross section is down by a factor of 10 approximately 12° off axis. The experimental data indicate a reduction in the received power of 10 approximately 0.17° off axis. Clearly, the scattered signal profile is not consistent with a classical Deirmendjian aerosol model. From reference 2 it is seen that for an assumed phase function distribution of

$$\begin{aligned} f(\theta) &= f(0) \left[1 - \frac{\theta}{\theta_0} \right] & 0 < \theta < \theta_0 \\ &= 0 & \theta \geq \theta_0 \end{aligned}$$

⁷Deirmendjian, D. Electromagnetic Scattering On Spherical Polydispersions, American Elsevier Publishing Co, Inc, New York, 1969

⁸Wells, W. Gal, G. and Munn, MW, Aerosol Distributions in Maritime Air and Predicted Scattering Coefficients in the Infrared, Applied Optics, vol 16, no 3, p 654-9, 1977

then

$$f(0) = \frac{3}{\pi \theta_0^2}$$

While this model for the forward scattering function is obviously overly simple, the dependence of $f(0)$ with θ_0 is important. If one relates θ_0 to the 10% points, then the measurements of 30 September 1976 indicate a θ_0 approximately 10 times smaller than from the M water haze that was assumed in the model. This again indicates an $f(0)$ approximately 100 times that assumed in the model. If $f(0)$ is increased by approximately 100 in the model, it is clear that good quantitative agreement is possible. While this agreement is clearly nonrigorous, the results are self-consistent.

Finally, the 1.06- μm data of 5 November 1976 (fig 16) can be examined. If the path loss of the 0.53- μm signal at zero transmitter elevation angle is compared with that of 25 February 1976, a value of β of 0.148 km^{-1} can be assumed (visibility of 26 km). If this value of β at 0.53 μm is scaled to 1.06 μm by using the empirical relation

$$\beta_{1.06 \mu\text{m}} = \frac{3.91}{V_{0.53 \mu\text{m}}} (1.927)^{-0.585(V_{0.53 \mu\text{m}})^{1/3}}$$

then $\beta_{1.06 \mu\text{m}} = 0.0482 \text{ km}^{-1}$ is determined. If this is used in the model with the $f(0)$ determined from Deirmendjian of $f(0^\circ; 1.06 \mu\text{m}) = 4$, then we calculate a path loss of -108 dB. The experimental value observed is -88 dB. Therefore, the model again under predicted the experiment by ~ 100 . This argument similarly lacks a rigorous base; however, the self-consistency of this result at 1.06 μm is important.

For the model used to determine communications system performance, a value of $f(0)$ approximately 80 times that predicted by Deirmendjian was used (fig 1). This is done both from self-consistency arguments just presented and also on the basis of empirical considerations. Even if there is no basis for the large $f(0)$, if the model is increased by ~ 80 , the results of the model do predict the experimental results.

SUMMARY

We have made measurements of propagation over the horizon by scattering from normal marine atmospheric aerosols. The measurements include propagation path losses and pulse distortion in the blue-green and at 1.06 μm . The model that has been developed is in reasonable agreement with the data. Further scattering measurements will be made. Design and construction of a one-way communication link between NELC and San Clemente Island (a distance of 128 km) are in progress. Figure 17 is a map showing details of this new propagation path.

REFERENCES

1. Atmospheric and Space Optical Communications for Naval Applications, Proceedings of 6th DoD Conference on Laser Technology, GC Mooradian, March 1974
2. NELC TR 1988, Extended Line of Sight Optical Communications Study, GC Mooradian, VJ Adrian, PH Levine, and WR Stone, June 1976
3. NRL Report 6152, Experimental Observations of Forward Scattering of Light in the Lower Atmosphere, JA Curcio and LF Drummeter, Jr, 30 September 1964
4. Over the Horizon Optical Communications Channel, Proceedings of Workshop on Remote Sensing of the Marine Boundary Layer, Vail, Colorado, GC Mooradian, M Geller, GJ Barstow, KE Davies, August 1976
5. Marine Weather of the World, McDonnell Douglas Report F-063, June 1968
6. NWC, China Lake, TN 4056-16, Weather Effects on Infrared Systems for Point Defense, FE Nicodemus, May 1972
7. Deirmendjian, D, Electromagnetic Scattering on Spherical Polydispersions, American Elsevier Publishing Co, Inc, New York, 1969
8. Wells, W, Gal, G, and Munn, MW, Aerosol Distributions in Maritime Air and Predicted Scattering Coefficients in the Infrared, Applied Optics, vol 16, no 3, p 654-9, 1977